

# Probing the ATP Hydrolysis Cycle of the ABC Multidrug Transporter LmrA by Pulsed EPR Spectroscopy

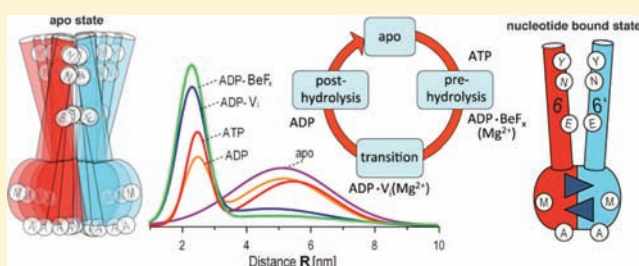
Ute A. Hellmich,<sup>†,§,⊥</sup> Sevdalina Lyubenova,<sup>‡,§,⊥</sup> Eva Kaltenborn,<sup>†,§</sup> Rupak Doshi,<sup>||</sup> Hendrik W. van Veen,<sup>||</sup> Thomas F. Prisner,<sup>\*,‡,§</sup> and Clemens Glaubitz<sup>\*,†,§</sup>

<sup>†</sup>Institute of Biophysical Chemistry, <sup>‡</sup>Institute of Physical and Theoretical Chemistry, and <sup>§</sup>Center for Biomolecular Magnetic Resonance, Goethe University Frankfurt, 60438 Frankfurt/M., Germany

<sup>||</sup>Department of Pharmacology, University of Cambridge, Cambridge CB2 1PD, United Kingdom

**S** Supporting Information

**ABSTRACT:** Members of the ATP binding cassette (ABC) transporter superfamily translocate various types of molecules across the membrane at the expense of ATP. This requires cycling through a number of catalytic states. Here, we report conformational changes throughout the catalytic cycle of LmrA, a homodimeric multidrug ABC transporter from *L. lactis*. Using site-directed spin labeling and pulsed electron–electron double resonance (PELDOR/DEER) spectroscopy, we have probed the reorientation of the nucleotide binding domains and transmembrane helix 6 which is of particular relevance to drug binding and part of the dimerization interface. Our data show that LmrA samples a very large conformational space in its apo state, which is significantly reduced upon nucleotide binding. ATP binding but not hydrolysis is required to trigger this conformational change, which results in a relatively fixed orientation of both the nucleotide binding domains and transmembrane helices 6. This orientation is maintained throughout the ATP hydrolysis cycle until the protein cycles back to its apo state. Our data present strong evidence that switching between two dynamically and structurally distinct states is required for substrate translocation.



## INTRODUCTION

Members of the ATP binding cassette (ABC) transporter superfamily translocate various types of molecules across the membrane at the expense of ATP. ATP hydrolysis takes place at the nucleotide binding domains (NBDs), which display strong sequence and structure similarities.<sup>1,2</sup> In contrast, substrate binding and translocation take place in the transmembrane domains (TMDs), which consist of  $\alpha$ -helical bundles with low sequence analogy, probably reflecting the diversity of transported substrates. The ABC architecture comprises two NBDs and two TMDs. These can be expressed on a single polypeptide or be assembled through homo- or heterodimerization of two half-transporters. In order to fulfill their function, the protein has to cycle through a number of catalytic states coupling ATP hydrolysis to substrate translocation. The observation that in particular ABC exporters crystallized to date share a common basic architecture has led to speculations whether their mode of action follows similar characteristics.<sup>3–5</sup> The ATP switch model, for example, suggests that substrate binding to a high-affinity binding site in the TMD triggers a conformational change, which is followed by ATP binding and NBD dimerization. As a result, a conformational change within the TMDs is induced facilitating substrate release at the opposite side of the plasma membrane. The structural and dynamic details of such a cycle are not yet fully understood, and it is under debate whether ATP binding

or hydrolysis triggers the conformational changes needed to drive substrate translocation.

In this study, site-directed spin labeling (SDSL) and pulsed electron–electron double resonance (PELDOR, also known as double electron–electron resonance, DEER) spectroscopy was used to follow conformational changes in LmrA during the catalytic cycle. LmrA is an ABC-transporter from *Lactococcus lactis* and a functional homologue of the essential human multidrug resistance P-glycoprotein (P-gp).<sup>6</sup> The gene for LmrA encodes a cysteine-free half-transporter with six transmembrane helices and a nucleotide binding domain on a single polypeptide that forms a functional homodimer.<sup>7</sup>

PELDOR allows the determination of distances in the range 20–80 Å.<sup>8,9</sup> It has become a widely used technique to investigate structural and dynamic aspects of biomacromolecules of arbitrary molecular weight<sup>10,11</sup> and has been shown to be especially useful for membrane proteins.<sup>12–14</sup> In the case of ABC transporters, PELDOR was utilized to monitor the effects of nucleotide binding on the *E. coli* Lipid A transporter MsbA<sup>15,16</sup> as well as the interaction of the substrate binding protein and nucleotides with MalGFK<sub>2</sub><sup>17</sup> extending previous cw-EPR studies.<sup>18–21</sup>

Received: November 23, 2011

Published: March 7, 2012

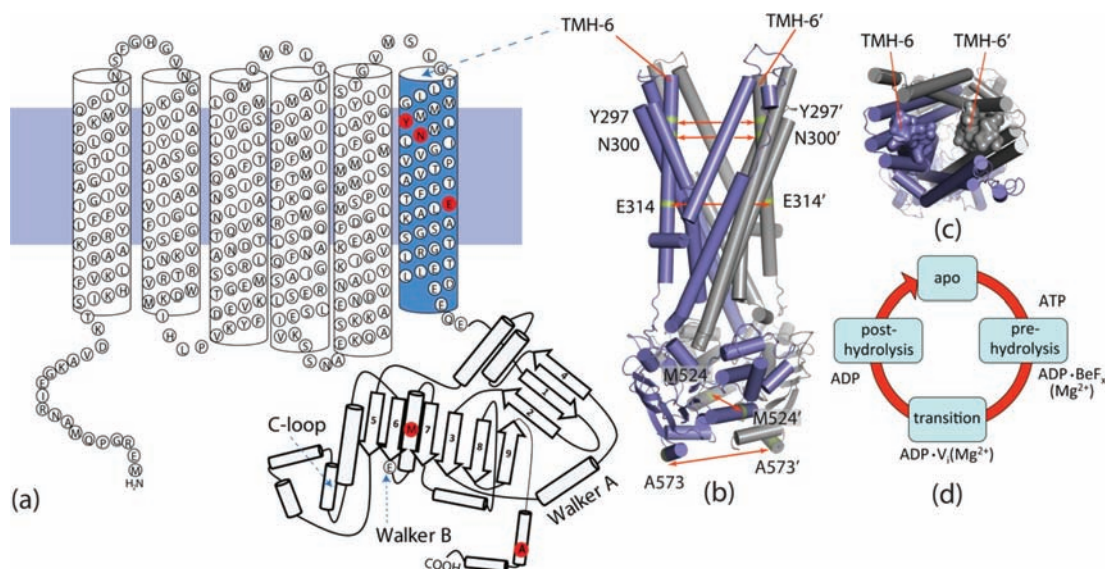


**Figure 1.** Topology plot of monomeric LmrA showing its six transmembrane helices and a soluble nucleotide binding domain (a). For site-directed spin-labeling, five single-cysteine mutants were prepared with cysteines at positions Y297, N300, E314, M524, and A573 (red). Wild type LmrA is cysteine-free. Since it is a homodimer, dipolar coupled spin pairs are created when using spin-labeled single-cysteine mutants. Their locations are indicated in a cartoon based on a homology model derived from Sav1866<sup>31</sup> (b). TMH6 forms part of the dimerization interface as visible in the top-view (c). Besides the apo state, pre- and posthydrolysis and transition states have been studied by trapping LmrA through the addition of different nucleotides and phosphate analogues (d). The topology is predicted on the basis of a comparison with the known 3D structure of Sav1866 [2HYD].<sup>31</sup> The homology model was built using SwissModel (swissmodel.expasy.org).

Here, we have introduced five single cysteine mutations into both the NBD (M524, A573) and transmembrane helix 6 (TMH6, Y297, N300, E314) (Figure 1a) of LmrA. Both TMH6s of homodimeric LmrA (corresponding to TMH6 and 12 in P-gp) are tethered to the NBDs, form part of the dimerization interface (Figure 1b,c), and have been described to be of particular relevance for drug recognition and binding.<sup>22–24</sup> Site-directed spin labeling of these mutants results in dipolar coupled spin pairs in the LmrA homodimer. Trapping different catalytic intermediate states of LmrA (Figure 1d) enabled us therefore to probe the conformational dynamics of an ABC transporter throughout its catalytic cycle.

## EXPERIMENTAL SECTION

**Materials.** Difco M17 medium was obtained from BD, Sparks, MD; n-dodecyl- $\beta$ -D-maltoside (DDM) from Applichem; Ni<sup>2+</sup>-nitriloacetic acid (NI-NTA) resin from Qjagen, Inc.; ATP, ADP, AMP-PNP, and (*N*-(1-oxyl-2,2,5,5-tetramethyl-3-pyrroindyl)iodoacetamide (IPSL) were obtained from Sigma. Beryllium fluoride was obtained from Acros Organics, and sodium ortho-vanadate from AppliChem. All other materials were reagent grade and obtained from commercial sources.

**Bacterial Strains and Growth Conditions.** *Lactococcus lactis* strain NZ9700 was used as a nisin producing strain. *L. lactis* strain NZ9000  $\Delta$ lmrA $\Delta$ lmrCD with plasmids pNHLmrA as a control and pNHLmrA Y297C, N300C, E314C, M524C, and A573C were used for expression of membrane protein. Precultures were grown without shaking at 30 °C overnight in M17 medium with 0.5% glucose and 5  $\mu$ g/mL chloramphenicol. Main cultures were grown at 30 °C without shaking to an OD<sub>660</sub> of 0.8. Cells were then induced with 1 mL per liter main culture of the supernatant of a *L. lactis* strain NZ9700 culture after centrifugation. Cells were grown for two hours and then harvested by centrifugation.

**Sample Preparation.** Inside-out vesicles (ISOV) were prepared as previously described.<sup>25</sup> Total membrane protein yield was determined with the colorimetric DC Protein Assay (Bio-Rad, Hertfordshire, U.K.) and detected at 750 nm with a UV 550 Jasco spectrophotometer. His-tagged protein was solubilized with 50 mM HEPES pH 8

with 1% n-dodecyl- $\beta$ -D-maltoside, 100 mM NaCl, and 10% glycerol for 1 h and then purified as described by us previously.<sup>25</sup> Pure protein yields were determined with the DC Protein Assay and verified with SDS-PAGE. For trapping with phosphate analogues, samples were incubated prior to spin labeling with 10 mM ATP, 7.5 mM MgSO<sub>4</sub>, and 5 mM sodium ortho-vanadate or beryllium fluoride, respectively. For trapping in the pre- or posthydrolysis state in the absence of phosphate analogues, samples were incubated prior to spin labeling with 10 mM ATP or 10 mM ADP, 7.5 mM MgSO<sub>4</sub>, respectively. For trapping with ATP in the presence of EDTA, samples were treated as described above but with 1 mM EDTA in all buffers. For trapping with AMP-PNP, samples were treated as described above, but incubated with 10 mM AMP-PNP, 7.5 mM MgSO<sub>4</sub> prior to spin labeling. Labeling was carried out overnight with 10-fold molar excess of IPSL on the NiNTA column. For removal of remaining free label, protein was washed with 30 column volumes. During washing, the glycerol content of washing buffer was stepwise increased from 10 to 20 v/v%. Samples were then eluted and concentrated to  $\sim$ 200  $\mu$ M before taking EPR measurements. The successful removal of excess of free IPSL from the samples was verified by cw EPR spectroscopy (Figure S4).

**EPR Spectroscopy.** Room temperature cw-EPR spectra were recorded on a Bruker ELEXSYS E-500 X-band spectrometer using a standard rectangular Bruker EPR cavity (ER4102T) equipped with an Oxford helium cryostat (ESR900). PELDOR experiments were performed using a Bruker ELEXSYS E-580 X-band spectrometer equipped with a standard Flexline probe head housing a dielectric ring resonator (MDS-W1) and an Oxford Instruments CF935 continuous flow helium cryostat with an ITC-5025 temperature controller. The second microwave frequency was coupled into the microwave bridge by a commercially available setup from Bruker (E580-400U). All experiments were carried out using the dead-time free four-pulse PELDOR sequence.<sup>26</sup> Typically, the signal was averaged for 16–20 h, depending on spin label concentrations, to obtain a sufficient signal-to-noise ratio. The pump pulse length ( $\pi$ ) was set to 12 ns at the resonance frequency of the resonator and applied to the maximum of the nitroxide spectrum, while the lengths of the probe pulses ( $\pi/2$ ) and ( $\pi$ ) were set to 32 ns and applied at 70 MHz higher frequency. The delay time between the first and second probe pulses was set to 136 ns and varied in 8 ns steps within 8 time intervals to

minimize contribution of proton nuclear modulation. The interpulse separation time between the second and third probe pulses was set either to 2040, 2540, or 2740 ns. There were 171, 212, or 229 data points taken, respectively, and a time increment of 12 ns was used. A two-step phase cycling was carried out on the  $\pi/2$  probe pulse to eliminate receiver offsets. All measurements were performed at a temperature of 40 K with a repetition rate of 0.25 kHz. The PELDOR time domain data were analyzed using custom fitting routines written in MatLab, taking spin concentration, spin labeling efficiency, and excitation efficiency directly into account. Spin concentrations and labeling efficiencies were verified by analyzing cw-EPR spectra (Figures S4, S5). These parameters are difficult to determine from our PELDOR data due to the short transversal relaxation time, which did not allow using a longer time window. Nevertheless, results from cw-EPR agreed well with the PELDOR analysis.

## RESULTS

We have carried out all EPR experiments with LmrA mutants solubilized in DDM, a membrane mimetic in which ATPase activity can be further stimulated by the addition of drugs.<sup>27</sup> EPR studies on related ABC transporters have shown that the conformational integrity of these systems is not compromised in detergent in comparison to liposomes.<sup>16</sup> DDM offers good sample stability, homogeneity, and favorable NBD accessibility, which is important for trapping different hydrolysis cycle intermediate states of LmrA. All DDM solubilized and spin labeled mutants showed an ATPase activity comparable to wild type LmrA (Figure S1), and transport activity was verified on inside-out vesicles (Figure S2), while CD spectroscopy showed native secondary structure of the preparation in DDM (Figure S3). Successful spin labeling was monitored by cw-EPR spectroscopy (Figure S4).

In order to emulate intermediate catalytic states of the ATP hydrolysis cycle of LmrA, a number of mimetics were utilized (Figure 1d): (i) The prehydrolysis state is represented by a LmrA-bound nucleotide such as ATP (in the absence of  $Mg^{2+}$ ) with a tetravalent terminal phosphorus atom and  $ADP \cdot BeF_x$  (in presence of  $Mg^{2+}$ ) with a tetravalent terminal beryllium atom. (ii) The transition state is emulated by  $ADP \cdot V_i(Mg^{2+})$  with a pentavalently bound terminal vanadium atom. (iii) The posthydrolysis state, which occurs after the release of  $P_i$ , is mimicked by binding of ADP to LmrA. (iv) The absence of all nucleotides and phosphate analogues yields the apo state that occurs between the release of  $P_i$  and ADP and before ATP binds again.

PELDOR time traces for all five LmrA mutants in all observed states are shown in Figure 2. These data were fitted either with a single or with a double Gaussian distance distribution. Intermolecular decay was taken into account by an exponential decay function for a statistical three-dimensional distribution of the protein dimers. The validity of this assumption was verified by a dilution experiment in which the protein concentration was halved (Figure S6). The Gaussian distance distribution functions obtained by this procedure are very similar to those obtained by Tikhonov regularization methods (Figure S7) and are chosen here because of enhanced clarity.

For the apo state, a monotonic PELDOR decay was observed for each of the five mutants, regardless of the spin-label position in NBD or TMH6. This decay does not result from intermolecular (i.e., dimer–dimer) spin–spin couplings but can be interpreted by a broad, weakly defined distance distribution described best by a single Gaussian (Figure S6).

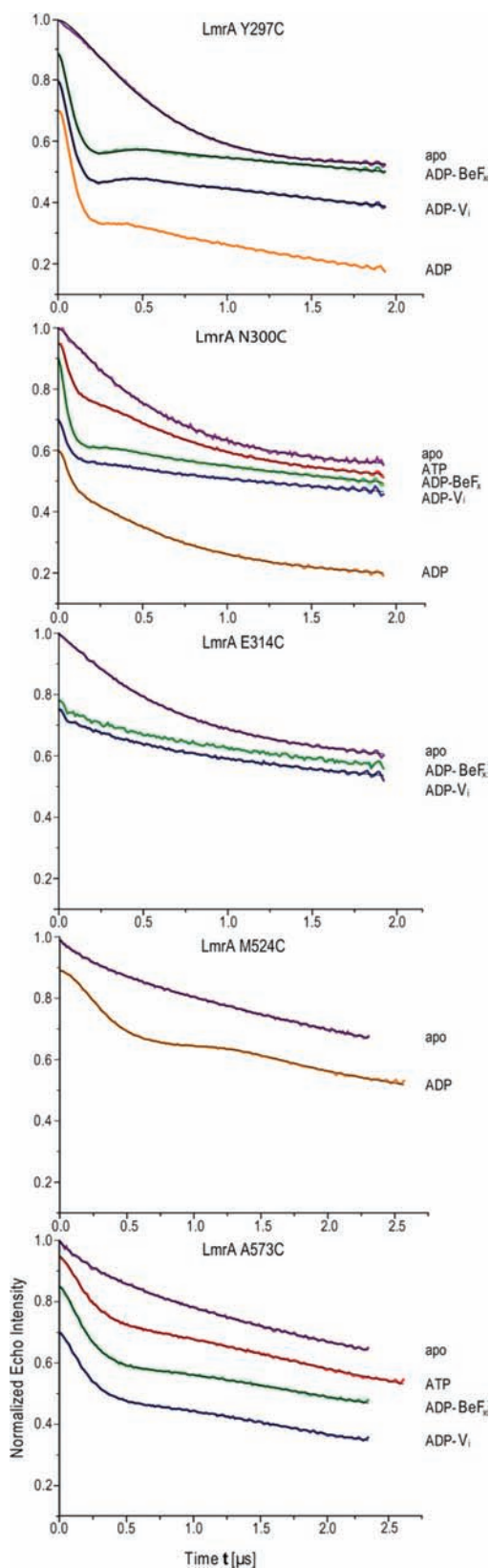


**Figure 2.** X-band PELDOR traces of LmrA N300C, Y297C, E314C, M524C, and A573C, recorded at 40 K. None of the apo state traces show dipolar oscillations resulting in broad distance distributions (Figure 3a). In contrast to the apo state, the nucleotide bound states show dipolar oscillations resulting in narrow distance distributions (Figure 3b). Simulations are shown in black on top of the PELDOR time traces. Note that especially for the apo-state the modulation

Figure 2. continued

depth and therefore the spin labeling efficiency cannot be read from the end of the PELDOR time traces directly, because of the broad distance distribution. Details to background correction and data analysis are given in the Experimental Section and as Supporting Information.

Corresponding distance distribution functions are shown in Figure 3a and cover a distance range from 20 to 80 Å.

In contrast to the apo state, all nucleotide bound states, by which catalytic intermediates were emulated, show dipolar oscillations in the PELDOR traces (Figure 2). Not all states were experimentally accessible for all mutants, because in some cases either sufficient spin labeling of a particular mutant in a certain state could not be obtained or a spin-labeled mutant could not be trapped in the desired state. However, an overall good coverage of the catalytic cycle has been achieved. The observed PELDOR traces result in narrow ( $\sigma = 2\text{--}9$  Å) and well-defined distance distributions (Figure 3b).

For TMH6 mutant LmrA Y297C, a mean distance of 27 Å is obtained for all nucleotide bound states, which shortens to 24 Å in LmrA N300C and to 18 Å in LmrA E314C. For LmrA N300C and E314C, optimal fits were achieved using two-Gaussian distance distributions, because a second population with a mean value of around 50 Å occurred occasionally in nucleotide bound states. This most likely arises from incomplete sample trapping and corresponds to an apo state fraction. The effect of nucleotide binding on the PELDOR data of the NBD mutants LmrA M524C and A573C also results in a narrow distance distribution in contrast to the apo state and in agreement with the observations made for TMH6. For LmrA M524C, only the ADP state could be trapped and at the same time sufficiently spin-labeled for PELDOR experiments. A mean distance of 40 Å was obtained for LmrA M524C in this state. For LmrA A573C, shorter mean distances of about 36 Å were observed upon nucleotide binding. The numerical parameters describing these Gaussian distance distributions are summarized in Tables S1 and S2.

## DISCUSSION

Our measurements for all mutants show that a significant narrowing of the interspin distance distributions is observed when progressing from the apo to prehydrolysis, transition, or posthydrolysis state. Surprisingly, all three nucleotide-bound intermediate states show very similar spin–spin distances within the resolution of the method. The distances obtained from the TMH6 mutants become smaller toward the core of the protein indicating that both TMH6 in the dimer are tilted with respect to each other and form an outwardly opened funnel.

The very broad distance distributions in the apo state of the investigated cysteine mutants reflect a significant orientational distribution of NBD and TMH6, which most likely results from large amplitude domain fluctuations whose ensemble is freeze-captured under the low temperature EPR conditions.<sup>14</sup> Similar EPR data have been observed for apo state MsbA.<sup>15,16</sup> The broad apo state distance distributions obtained here cover the whole conformational space defined by different crystal structures of apo state P-glycoprotein<sup>22</sup> as well as by the open and closed MsbA<sup>28</sup> apo state structures (Table S1). Our data also agree with our previous solid-state NMR study on LmrA in which highly flexible NBDs in the apo state and

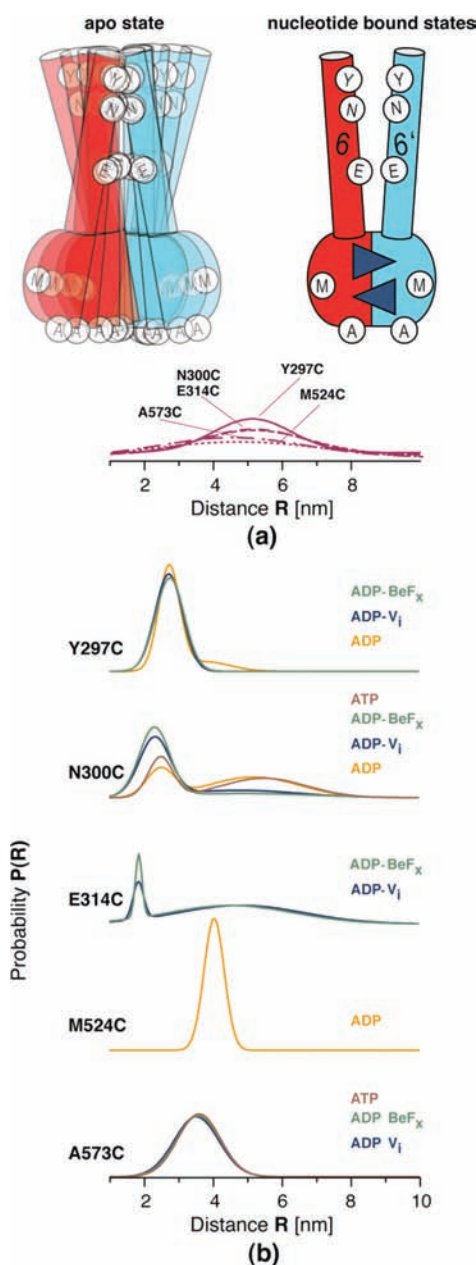


**Figure 3.** Distance distributions calculated from PELDOR traces shown in Figure 2. For the apo state, broad distributions covering a range from 20 to 80 Å were obtained for all five mutants (a). Upon nucleotide binding, all distribution functions become narrow both for inter-TMH6 and inter-NBD distances. The observed mean distances are in agreement with dimerization of NBDs and formation of an outward facing funnel shaped conformation of TMH6. PELDOR traces could be fitted best with single Gaussian distributions except for some states of LmrA N300C and E314C which were described best by two Gaussians and did contain an apo-state contribution probably caused by incomplete trapping. Parameters of the Gaussian distance distributions are summarized in Tables S1 and S2.

reduced mobility on the nucleotide bound state have been described.<sup>29</sup> Indeed, a highly dynamic apo state might be a functional prerequisite for LmrA to recognize a large variety of substrates through a conformational selection mechanism. This concept of a dynamic apo state and its relevance for substrate binding has gained importance over the past decade for a number of different proteins.<sup>30</sup>

Nucleotide binding has significant structural and dynamic consequences on both NBDs and TMDs. The reduced width of the observed distance distributions means that conformational space of both domains is significantly reduced compared to the apo state. The observed NBD-NBD distances upon nucleotide binding are in agreement with dimerization of these domains. At the same time, both TMH6s orient in an outwardly opened funnel-like conformation (Figure 3). The distances obtained here for LmrA are compatible with the nucleotide bound state X-ray structures of MsbA and Sav1866 (Table S2),<sup>28,31,32</sup> which shows that there is a structural similarity between these different ABC export systems as predicted previously based on functional overlap.<sup>33,34</sup> The data presented here for LmrA agree very well with the conformational changes required for an alternating access functional model for ABC exporters.<sup>15,16,35</sup> For this model, switching between an open conformation and a closed one with dimerized NBDs is required and triggered by nucleotide binding or release to or from the NBDs.<sup>4,15,16,36</sup>

The high similarity between prehydrolysis, transition, and posthydrolysis catalytic intermediate states indicate that one major conformational change is triggered by ATP binding, while only small rearrangements are required to complete the transport and hydrolysis cycles: NBD closure and the formation of an outward facing orientation of TMH6 in LmrA occurs in the emulated prehydrolysis state (ATP or ADP·BeF<sub>x</sub> (Mg<sup>2+</sup>)), which could be prepared for all mutants except for LmrA M524C. This means that switching from the flexible apo to the more restrained nucleotide bound state conformation is triggered by ATP binding and does not rely on hydrolysis. For ATP hydrolysis to occur, the presence of Mg<sup>2+</sup> is required. In principle, residual divalent ions in the buffer could also allow LmrA to hydrolyze ATP, which would lead unintentionally to the formation of a transition or posthydrolysis instead of a prehydrolysis state. However, additional control experiments in the presence of EDTA and AMP-PNP(Mg<sup>2+</sup>) did allow us to exclude this possibility (Figure S8). Besides its requirement for hydrolysis, the presence of Mg<sup>2+</sup> has been widely discussed to be needed for the NBDs to dimerize.<sup>37</sup> Conflicting data has been presented showing that for example P-gp and BmrA do require Mg<sup>2+</sup> for NBD dimerization, whereas MalGFK<sub>2</sub> needs both ATP and the maltose binding protein, but not Mg<sup>2+</sup>.<sup>38–40</sup> For MRP3, ATP-dependent dimerization of NBDs in the absence of divalent cations has also been proposed.<sup>41</sup> Our data clearly show that Mg<sup>2+</sup> is not a requirement for NBD dimerization and TMH6 reorientation in LmrA in the presence of ATP.

Interestingly, we observe that in LmrA, ADP binding triggers NBD dimerization and TMH6 reorientation the same way as all the other nucleotides/nucleotide analogues. This is somewhat unexpected, because it was found in crystallized isolated NBDs that the  $\gamma$ -phosphate of ATP is required to keep the NBDs dimerized, which dissociate upon ATP hydrolysis.<sup>42</sup> Our observations mean that both P<sub>i</sub> and ADP release and not just hydrolysis would be required to complete the catalytic cycle by NBD dissociation. The structural implications of ADP binding to LmrA agree with the crystal structure of ADP-bound, outward facing Sav1866 with dimerized NBDs.<sup>31</sup> Although detergent induced conformational effects have not been ruled out by the authors of that study,<sup>32</sup> LmrA is known to be active in detergent and shows stimulated ATPase activity,<sup>27</sup> which requires highly specific cross talk between TMD and NBD.

## CONCLUSION

The possibility to measure long-range conformational changes by PELDOR offers unique insight into the functional mechanism of ABC transporters which complements and completes knowledge derived from 3D crystal structures. Our experiments show that LmrA samples a very large conformational space in its apo state, which is significantly reduced upon nucleotide binding: the NBDs dimerize and TMH6 adopts an outwardly open conformation. The orientation of both NBD and TMH6 remains almost the same in all the nucleotide bound states during the remainder of the catalytic cycle within the resolution of our method. On the basis of these findings, one could speculate that efficient substrate translocation only requires switching between two dynamically and structurally distinct states. In the ATP-hydrolysis cycle, ATP binding and ADP/P<sub>i</sub> release are the key steps: ATP binding triggers the grand transition from a highly flexible apo state to a significantly conformationally restricted state (that could temporally concur with the substrate release) and ADP/P<sub>i</sub> release is required for resetting the transporter to its apo state. This might be a general feature of the functional mechanism of ABC multidrug efflux pumps.

## ASSOCIATED CONTENT

### Supporting Information

Transport activity of LmrA mutants, ATPase activity of spin-labeled LmrA mutants, CD spectroscopy, cw-EPR, PELDOR control experiments. This material is available free of charge via the Internet at <http://pubs.acs.org>.

## AUTHOR INFORMATION

### Corresponding Author

prisner@chemie.uni-frankfurt.de; glaubit@chemie.uni-frankfurt.de

### Author Contributions

<sup>†</sup>These authors contributed equally.

### Notes

The authors declare no competing financial interest.

## ACKNOWLEDGMENTS

We acknowledge support by the DFG through SFB 807 "Transport and Communication across Membranes". We thank Reza Dastvan and Leonie Mönkemeyer for help with control experiments and for setting up trapping conditions and Lena Buchner for valuable discussions.

## REFERENCES

- (1) Davidson, A. L.; Maloney, P. C. *Trends Microbiol.* **2007**, *15*, 448–55.
- (2) Jones, P. M.; O'Mara, M. L.; George, A. M. *Trends Biochem. Sci.* **2009**, *34*, 520–31.
- (3) Oldham, M. L.; Davidson, A. L.; Chen, J. *Curr. Opin. Struct. Biol.* **2008**, *18*, 726–33.
- (4) Dawson, R. J.; Hollenstein, K.; Locher, K. P. *Mol. Microbiol.* **2007**, *65*, 250–7.
- (5) Linton, K. J.; Higgins, C. F. *Pflugers Arch* **2007**, *453*, 555–67.
- (6) van Veen, H. W.; Venema, K.; Bolhuis, H.; Oussenko, I.; Kok, J.; Poolman, B.; Driessen, A. J.; Konings, W. N. *Proc. Natl. Acad. Sci. U.S.A.* **1996**, *93*, 10668–72.
- (7) van Veen, H. W.; Margolles, A.; Muller, M.; Higgins, C. F.; Konings, W. N. *EMBO J.* **2000**, *19*, 2503–14.
- (8) Milov, A. D.; Salikhov, K. M.; Shirov, M. D. *Fiz. Tverd. Tela* **1981**, *23*, 975–982.

- (9) Martin, R. E.; Pannier, M.; Diederich, F.; Gramlich, V.; Hubrich, M.; Spiess, H. W. *Angew. Chem., Int. Ed.* **1998**, *37*, 2834–2837.
- (10) Jeschke, G.; Polyhach, Y. *Phys. Chem. Chem. Phys.* **2007**, *9*, 1895–1910.
- (11) Schiemann, O.; Prisner, T. F. *Q. Rev. Biophys.* **2007**, *40*, 1–53.
- (12) Altenbach, C.; Kusnetzow, A. K.; Ernst, O. P.; Hofmann, K. P.; Hubbell, W. L. *Proc. Natl. Acad. Sci. U.S.A.* **2008**, *105*, 7439–7444.
- (13) Dockter, C.; Volkov, A.; Bauer, C.; Polyhach, Y.; Joly-Lopez, Z.; Jeschke, G.; Paulsen, H. *Proc. Natl. Acad. Sci. U.S.A.* **2009**, *106*, 18485–18490.
- (14) Mchaourab, H. S.; Steed, P. R.; Kazmier, K. *Structure* **2011**, *19*, 1549–61.
- (15) Borbat, P. P.; Surendhran, K.; Bortolus, M.; Zou, P.; Freed, J. H.; McHaourab, H. S. *PLoS Biol.* **2007**, *5*, e271.
- (16) Zou, P.; Bortolus, M.; McHaourab, H. S. *J. Mol. Biol.* **2009**, *393*, 586–97.
- (17) Grote, M.; Polyhach, Y.; Jeschke, G.; Steinhoff, H. J.; Schneider, E.; Bordignon, E. *J. Biol. Chem.* **2009**, *284*, 17521–6.
- (18) Do Cao, M. A.; Crouzy, S.; Kim, M.; Becchi, M.; Cafiso, D. S.; Di Pietro, A.; Jault, J. M. *Protein Sci.* **2009**, *18*, 1507–20.
- (19) Dong, J.; Yang, G.; McHaourab, H. S. *Science* **2005**, *308*, 1023–8.
- (20) Goetz, B. A.; Perozo, E.; Locher, K. P. *FEBS Lett.* **2009**, *583*, 266–70.
- (21) Orelle, C.; Alvarez, F. J.; Oldham, M. L.; Orelle, A.; Wiley, T. E.; Chen, J.; Davidson, A. L. *Proc. Natl. Acad. Sci. U.S.A.* **2010**, *107*, 20293–8.
- (22) Aller, S. G.; Yu, J.; Ward, A.; Weng, Y.; Chittaboina, S.; Zhuo, R.; Harrell, P. M.; Trinh, Y. T.; Zhang, Q.; Urbatsch, I. L.; Chang, G. *Science* **2009**, *323*, 1718–22.
- (23) Pleban, K.; Kopp, S.; Csaszar, E.; Peer, M.; Hrebicek, T.; Rizzi, A.; Ecker, G. F.; Chiba, P. *Mol. Pharmacol.* **2005**, *67*, 365–74.
- (24) Smriti; Zou, P.; McHaourab, H. S. *J. Biol. Chem.* **2009**, *284*, 13904–13.
- (25) Hellmich, U. A.; Haase, W.; Velamakanni, S.; van Veen, H. W.; Glaubitz, C. *FEBS Lett.* **2008**, *582*, 3557–62.
- (26) Pannier, M.; Veit, S.; Godt, A.; Jeschke, G.; Spiess, H. W. *J. Magn. Reson.* **2000**, *142*, 331–340.
- (27) Venter, H.; Velamakanni, S.; Balakrishnan, L.; van Veen, H. W. *Biochem. Pharmacol.* **2008**, *75*, 866–874.
- (28) Ward, A.; Reyes, C. L.; Yu, J.; Roth, C. B.; Chang, G. *Proc. Natl. Acad. Sci. U.S.A.* **2007**, *104*, 19005–10.
- (29) Sjarheyeva, A.; Lopez, J. J.; Lehner, I.; Hellmich, U. A.; van Veen, H. W.; Glaubitz, C. *Biochemistry* **2007**, *46*, 3075–83.
- (30) Kern, D.; Zuiderweg, E. R. P. *Curr. Opin. Struct. Biol.* **2003**, *13*, 748–757.
- (31) Dawson, R. J.; Locher, K. P. *Nature* **2006**, *443*, 180–5.
- (32) Dawson, R. J.; Locher, K. P. *FEBS Lett.* **2007**, *581*, 935–8.
- (33) Reuter, G.; Janvilisri, T.; Venter, H.; Shahi, S.; Balakrishnan, L.; van Veen, H. W. *J. Biol. Chem.* **2003**, *278*, 35193–35198.
- (34) Velamakanni, S.; Yao, Y.; Gutmann, D. A. P.; van Veen, H. W. *Biochemistry* **2008**, *47*, 9300–9308.
- (35) Zou, P.; McHaourab, H. S. *J. Mol. Biol.* **2009**, *393*, 574–85.
- (36) Lee, J. Y.; Urbatsch, I. L.; Senior, A. E.; Wilkens, S. *J. Biol. Chem.* **2008**, *283*, 5769–79.
- (37) Hellmich, U. A.; Glaubitz, C. *Biol. Chem.* **2009**, *390*, 815–34.
- (38) Buchaklian, A. H.; Klug, C. S. *Biochemistry* **2005**, *44*, 5503–9.
- (39) Hrycyna, C. A.; Ramachandra, M.; Germann, U. A.; Cheng, P. W.; Pastan, I.; Gottesman, M. M. *Biochemistry* **1999**, *38*, 13887–99.
- (40) Orelle, C.; Dalmás, O.; Gros, P.; Di Pietro, A.; Jault, J. M. *J. Biol. Chem.* **2003**, *278*, 47002–8.
- (41) Hoffman, A. D.; Urbatsch, I. L.; Vogel, P. D. *Protein J.* **2010**, *29*, 373–379.
- (42) Smith, P. C.; Karpowich, N.; Millen, L.; Moody, J. E.; Rosen, J.; Thomas, P. J.; Hunt, J. F. *Mol. Cell* **2002**, *10*, 139–149.